FAULT DETECTION USING STATE ESTIMATION AND MACHINE CURRENT SIGNATURE ANALYSIS

Lavinius Ioan Gliga[1], Dumitru Popescu[2], Houcine Chafouk[3]

Gearless wind turbines can be outfitted with Permanent Magnet Synchronous Generators. These may be affected by impairments. Machine Current Signature Analysis can be utilized to find these faults, as they insert additional harmonics. These manifestations also exist in the residuals of the generated currents, calculated via an Extended Kalman Filter. The Fast Fourier Transform is utilized to compute the residuals spectrum, to find these supplementary harmonics. In this work, the Goertzel Filter is proposed as a better substitute to the Fast Fourier Transform, for the fault detection of such a generator. The Goertzel Filter was implemented in MATLAB / Simulink and the obtained outcomes confirm its effectiveness. Moreover, a method to estimate the covariance matrix of process noise is briefly presented. This matrix is necessary for the implementation of a Kalman filter.

Keywords: Permanent Magnet Synchronous Generator, Extended Kalman Filter, Fast Fourier Transform, Goertzel Filter, Fault Detection

1. Preliminaries

1.1. Introduction

Gearless Wind Turbines (GWTs) are outfitted with a Permanent Magnet Synchronous Generator (PMSG). Even though current GWTs are more dependable than earlier ones, they may nevertheless malfunction. Thus, they need automated fault detection systems. The sub-assemblies which may break down in a GWT are the propeller blades, the PMSG, the rotor shaft, etc., [17]. The PMSG, which is dealt with in this work, is culpable for approximately 25% of the downtime of a GWT. The percentages of breakdown and caused downtime due to GWT sub-systems are shown in [10].

The generated currents can pinpoint to faults that occur in the PMSG. The approach based on the inspection of these signals is called Machine Current Signature Analysis (MCSA).

[1]Teaching Assistant, Faculty of Automatic Control and Computer Science, "Politehnica" University of Bucharest, Romania, e-mail: lavinius.gliga@ieee.org

[2]Professor, Faculty of Automatic Control and Computer Science, "Politehnica" University of Bucharest, Romania

[3]Professor, IRSEEM, ESIGELEC, UniRouen, Normandy University, France

The Fast Fourier Transform (FFT) is used when impairments insert supplementary harmonics into the acquired measurements. The FFT is used to calculate the spectrum of a signal across all conceivable frequencies. This is not effective when just several frequencies are concerned. To optimize the fault detection algorithm, the authors selected the Goertzel Algorithm (GA) [11]. It is implemented as a series connection between a Finite Impulse Response (FIR) filter and an Infinite Impulse Response (IIR) one. The GA is utilized to assess the magnitude of a signal at a specific value of the frequency. Due to the reduced number of considered frequencies in the fault detection of a PMSG, the GA is suitable for this scenario.

The novelty of this paper is in the replacement of the FFT with the Goertzel Filter, for the fault diagnosis of the PMSG of a GWT.

A literature survey on similar papers is presented in Section II. The PMSG model is shown in Section III. The specific implementation of the EKF is described in Section IV. The GA is shown in Section V. The most common PMSG faults are listed in Section VI. The results obtained in simulation are presented and disseminated in Section VII. This work is closed by the conclusions and the perspectives.

1.2. Literature Survey

In [2], the acceleration of a structure is monitored using the GA. It was chosen as the transducers are powered using batteries, thus there is a low amount of available electrical energy.

The GA is utilized in [13] to compute the Total Harmonics Distortion of an electrical current that flows through a part of a smart grid. The GA was coded on a low-power smart meter.

In [6], two GAs are used in parallel, to assure the redundancy required in a fault tolerant system. This approach is not discussed in this work, but it may be appropriate in critical application, such as nuclear power plants.

The GA was utilized, in [18], to find eccentricity faults in a three-phase induction electrical machine. The authors of that paper also used the MCSA approach. However, in this work, five possible defects of a PMSG are dealt with.

In [19], the FFT was supplanted by a sliding-window FFT (SWFFT), which was inspired by the GA. The SWFFT was used to calculate the magnitude of only one frequency component of the signal. The SWFFT was utilized to find eccentricity-type failures that can affect an induction motor.

The contribution is the usage of a GA for the diagnosis of a PMSG used in GWTs. This wirk built upon previous ones shown in [9] and [10].

2. The Model of the Generator

A GWT comprises:

- a rotor, which is made up of the propeller and its hub;

- a main shaft that connects the rotor to the PMSG;
- a permanent magnet synchronous generator;
- a full-power converter, which comprises:
  - a rectifier;
  - a capacitor on the direct current link;
  - an inverter;
- a bank of filters used to smooth-out the generated sinusoidal wave;
- a transformer;
- a connection to the external electrical grid.

The PMSG was simulated in MATALB / Simulink utilizing the Simscape/Power Systems toolbox. The model of the PMSG is [8]:

$$\hat{\dot{I}}_d(t) = -\frac{R_s I_d(t)}{L_s} + \frac{n_p \omega_m(t) L_s I_q(t)}{L_s} + \frac{V_d(t)}{L_s}, \tag{1}$$

$$\hat{\dot{I}}_q(t) = -\frac{R_s I_q(t)}{L_s} - \frac{n_p \omega_m(t) L_s I_d(t)}{L_s} - \frac{n_p \omega_m(t) \phi}{L_s} + \frac{V_q(t)}{L_s}, \tag{2}$$

where I_d, I_q, V_d and V_q are the currents (in A) and the voltages (in V) in the dq0 rotor frame. R_s and L_s are the stator resistance (in Ω) and inductance (in H) in the dq0 frame. ω_m is the angular velocity of the generator shaft (in rpm), and ϕ is flux linkage between the permanent magnet rotor and the stator (in Wb).

The model states are the generated currents. The inputs are the voltages and the angular velocity. The model is nonlinear, due of the multiplication of a state and an input, in each equation.

3. **The Extended Kalman Filter**

Research was conducted on generator fault diagnosis and performance monitoring via MCSA ([16]) ([21]), to eliminate the need for dedicated sensors. However, the generated currents are affected by the change in wind speed and the results obtained from signal processing methods, like the Fast Fourier Transform, can be erroneous ([4]).

A possible solution is to generate residuals between the real currents and the estimated ones [9]. A state estimator can be used to ensure the required redundancy. The challenge, when using a state estimator, is to find out the covariance matrices for the process and for the measurement noises. If the matrices are not properly chosen, the estimated states might not converge to the real ones.

The solution, as shown in [7], is to use an iterative method which could be implemented online. The covariance matrix can be automatically adapted to always ensure the consistency of the estimated states. The method is simple to utilize, but its usage is constrained to certain non-linear systems.

The classical formulation of the EKF is [7]

$$\hat{x}_{k+1} = f(\hat{x}_k, u_k), \tag{3}$$

$$y_k = h(\hat{x}_k), \tag{4}$$

where the state function is $f : \mathbb{R}^{n_x+n_u} \to \mathbb{R}^{n_x}$ and the measurement function is $h : \mathbb{R}^{n_x} \to \mathbb{R}^{n_y}$. For the EKF, the model presented in (1) and (2) is already written in the required form. The algorithm of the EKF is ([5]):

- Prediction phase:

$$\hat{P}_k = F_k \hat{P}_{k-1} F_k^T + Q_k; \tag{5}$$

- Update phase:

$$K_k = \hat{P}_k H_k^T (H_k \hat{P}_k H_k^T + R_k)^{-1}; \tag{6}$$

$$\hat{x}_k^* = \hat{x}_k + K_k * (y_k - \hat{y}_k); \tag{7}$$

$$\hat{P}_k^* = (I - K_k H_k)\hat{P}_k; \tag{8}$$

where $F \in \mathbb{R}^{n_x * n_x}$ and $H \in \mathbb{R}^{n_y * n_x}$ are the Jacobians of the state and measurement functions.

The measurement noise covariance matrix can be easily estimated ([14]). The measurement noise affects the data through the sensors. Information about this perturbation is available in the sensor datasheet, as the sensor tolerance or precision. This is the standard deviation of the measurements of the sensor. Thus, the covariance matrix can be computed as:

$$R = \begin{bmatrix} \sigma_1^2 & 0 & \dots & 0 \\ 0 & \sigma_2^2 & \dots & 0 \\ \vdots & \vdots & \ddots & \vdots \\ 0 & 0 & \dots & \sigma_n^2 \end{bmatrix},$$

where $\sigma_i, i = \{1, 2, ..., n_y\}$ is the standard deviation on each measurement channel. This matrix is diagonal because there is a single sensor on each measurement channel. Therefore, the data acquired by each sensor is only affected by the noise which perturbs that channel.

The estimation of the process noise covariance matrix is [7]

$$Q_k = A^{-1} \left(c\hat{o}v \left(\epsilon_k, \epsilon_k \right) - R \right) \left(A^{-1} \right)^T. \tag{9}$$

The drawbacks of this method are:

- $h : R^{n_x} \to R^{n_y}$ must be a linear function defined as $h(x) = Ax + b$, where $A \in R^{n_y * n_x}$ is an invertible matrix and $b \in R^{n_y}$ is a vector. Since A is invertible, it is a square matrix and $n_y = n_x$.
- The estimation error between the real and the estimated states should tend to zero, i.e. $\lim_{k \to \inf} (x_k - \hat{x}_k) = 0$.

The covariance matrix of the estimation error can be computed online using ([3])

$$c\hat{o}v \left(\epsilon_k, \epsilon_k \right) = c\hat{o}v \left(\epsilon_{k-1}, \epsilon_{k-1} \right) - \frac{c\hat{o}v \left(\epsilon_{k-1}, \epsilon_{k-1} \right) - \left(\epsilon_k - \bar{\epsilon}_k \right) \left(\epsilon_k - \bar{\epsilon}_k \right)^T}{k}, \tag{10}$$

where $\bar{\epsilon}_k$ is the mean of the estimation error, computed at sampling time k.

4. The Goertzel Algorithm

The GA is utilized to calculate the Discrete Fourier Transform (DFT) in a single frequency bin, i.e., the interval between two frequencies values.

The stable version of the GA, that is considered in this paper, is [20]:

$$H_{GA}(z^{-1}) = \frac{1 - e^{-j2\pi\frac{k}{N}}z^{-1}}{1 - 2\cos\left(2\pi\frac{k}{N}\right)z^{-1} + z^{-2}}. \tag{11}$$

This transfer function has one zero at $e^{-j2\pi\frac{k}{N}}$ and two complex conjugate poles at $e^{\pm j2\pi\frac{k}{N}}$. All poles and zeros are located on the unit circle. It is possible to show that the transfer function is stable [20], [15]. Just very large round-off errors (that may arise when filtering a long series of values) can destabilize it.

The GA is implemented on digital equipment by using the equations:

$$v[n] = 2\cos\left(2\pi\frac{k}{N}\right)v[n-1] - v[n-2] + x[n], \tag{12}$$

$$y[n] = v[n] - e^{-j2\pi\frac{k}{N}}v[n-1], \tag{13}$$

where v is an internal variable, x is the input, y is the output and n is the sampling moment.

To avoid the complex number multiplication from (13), the output can be changed, to be the square of the magnitude in the considered frequency bin. Thus, the output will be [10]:

$$y[n]|_{n=N} = v^2[n-1] + v^2[n] - 2v[n-1]v[n]\cos\left(2\pi\frac{k}{N}\right). \tag{14}$$

The implementation of the GA utilizing two difference equations, is called the Goertzel Filter (GF). To maintain the stability of the GF when filtering a long seris of values, its internal value must be reset to 0 after each calculation of the output [15]. The output of the filter is only calculated every N sampling moments.

5. An Overview of Considered Faults

The common faults of a PMSG introduce harmonics into the generated currents. These impairments, and their associated inserted harmonics, are [1]:

(1) demagnetization fault (DMF) happens when the rotor loses at least some of its residual magnetic flux. The symptoms of DMF are harmonics which appear at the frequencies $f_{i_{DMF}} = (1 \pm \frac{2m-1}{n_P})f_{ABC}$.

(2) inter-turn short circuit (ISCF) appears when a current crosses two turns of the stator winding, that belongs to one phase. Its symptoms are harmonics introduced at the frequencies $f_{i_{ISCF}} = (2m+1)f_{ABC}$.

(3) eccentricity fault occurs when the rotational axis of the rotor is not properly centered. There are three types of eccentricity faults:

Table 1

Frequencies of Introduced Harmonics

Faults	Frequencies	Signal
SEF	25	Generated Currents
DEF	58.33	Generated Currents
ISCF	250	Generated Currents

(a) static eccentricity fault (SEF) - the deviation in the air gap is constant. It inserts harmonics at the frequencies $f_{i_{SEF}} = (1 - \frac{3}{n_P})f_{ABC}$ and $f_{i_{DEF}} = (1 + \frac{1}{n_P})f_{ABC}$, where f_{ABC} is the frequency of the generated current. ;

(b) dynamic eccentricity fault (DEF) - the deviation in the air gap changes in time. Its symptoms are harmonics at the frequencies $f_{i_{DEF}} = (1 + \frac{1}{n_P})f_{ABC}$;

(c) mixed eccentricity fault (MEF) - both of the above.

The fault signature matrix is shown in [9]. All impairments insert harmonics in the generated current, so MCSA can be used for fault detection. Not all faults can be isolated from each other (e.g. eccentricity-type faults and DMF), because they introduce harmonics at similar frequencies.

In MCSA, the FFT is utilized to check for the harmonics that may be present in the generated currents. Nevertheless, the GF may also be employed for this task. Several GFs must be used in parallel - one for each frequency of interest [12]. In this work, only SEF, DEF and ISCF are considered (as DMF introduces the same harmonics). Therefore, three GFs are run in parallel: GF I to detect SEF, GF II to detect DEF and GF III to detect ISCF.

6. **Simulation and Results**

The faults inserted the following symptoms into the different acquired signals are shown in Table 1.

The frequencies of the harmonics were calculated by assuming that the generated three-phase currents would have a frequency of 50Hz. All harmonics had an amplitude of 0.05 A, to test GF in the case of incipient faults.

Several parameters were pre-calculated to hasten the GFs:

- The sampling period was $1e^{-6}$ sec, to assure the stability of the simulated model (a constraint imposed by the Simscape/Power Systems toolbox).
- Various numbers of frequency bins were chosen:
  - $N = 100000$ bins were utilized for SEF and DEF detection. Thus, each bin comprises 10 frequencies that may be represented using integers.

  - $N = 10000$ bins were chosen for ISCF. Each bin covers 100 frequencies representable utilizing integers.
- The bins of interest were chosen at $k = \left[0.5 + \frac{N*f_i}{f_s}\right]$, where k is rounded to the nearest integer.
- The cosine from (12) was pre-calculated.

The different numbers of frequency bins were used to design the three different GFs: one for SEF detection, one for DEF detection and another one for ISCF detection. The input of each GF were the residuals computed between the generated and the estimated currents. By considering N, f_i and computing k, each GF was designed to output the harmonic content inside a frequency interval centered around a certain f_i. New values were input in each GF at each sampling moment (i.e. when the values of the current were measured and new residuals were computed). The three different GFs ran in parallel.

Simulation results from when SEF affects the PMSG are shown in Figures 1 to 3. The squared magnitude of the inserted harmonic is noticeable on the output of GF II, where its value is almost 1500. The other two GSs output a squared magnitude of around 150, and respectively 30.

Simulation results from when DEF affects the generator are shown in Figures 4 to 6. The output of GF II went up to the order of thousands. The other two filters output squared magnitudes of hundreds, and tens of Ampers.

The ISCF was inserted alongside the DEF. While GF I shows a squared magnitude in the order of hundreds, the output of GF II remains in the order of thousands, while GF III reports a squared magnitude in the order of hundreds.

The output of GF III was peculiar because it seemed to have a rising trend. The others seemed to have a constant or near constant output. We simulated GF III for a long period, in the presence of just the ISCF since it caused an increase in the squared magnitude. It appears that the output is modulated in amplitude by a sinusoid with a very low frequency.

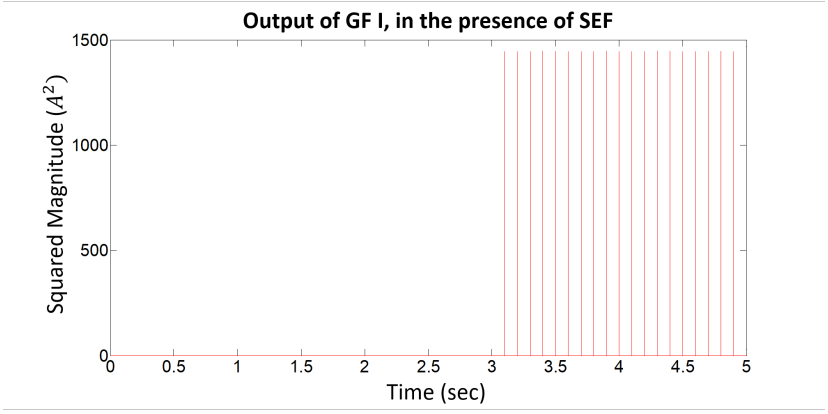

Fig. 1. The output of GF I, in the presence of SEF

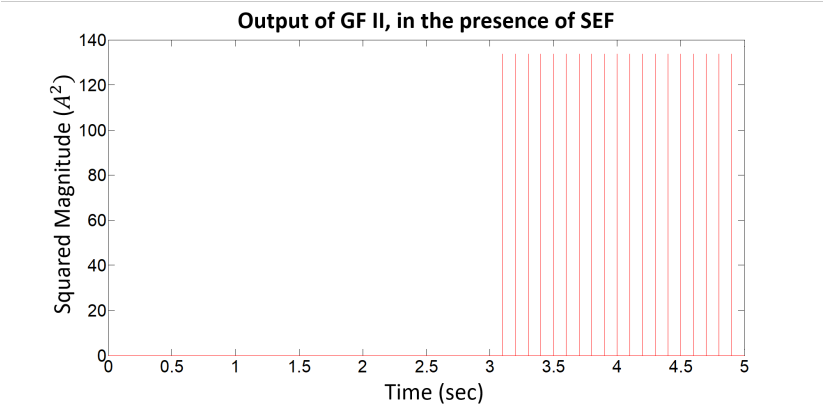

Fig. 2. The output of GF II, in the presence of SEF

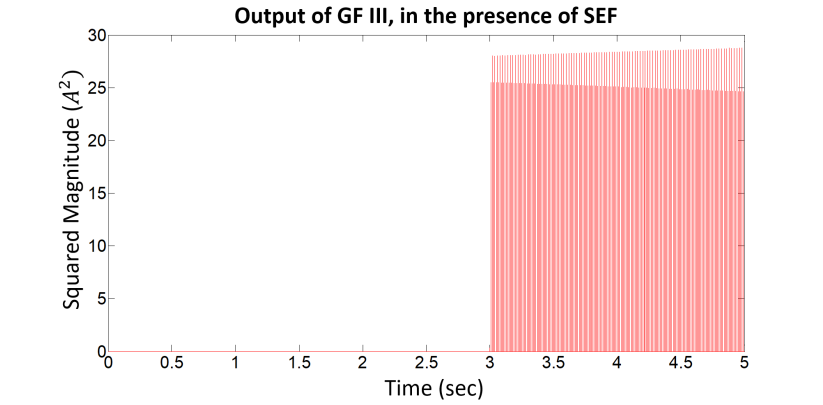

Fig. 3. The output of GF III, in the presence of SEF

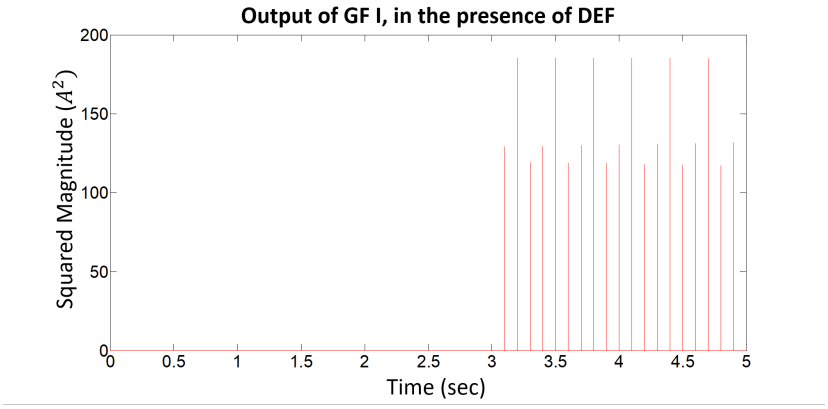

Fig. 4. The output of GF I, in the presence of DEF

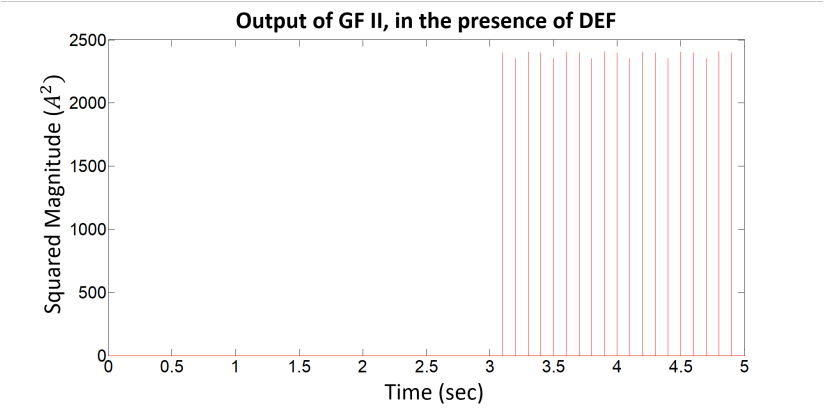

Fig. 5. The output of GF II, in the presence of DEF

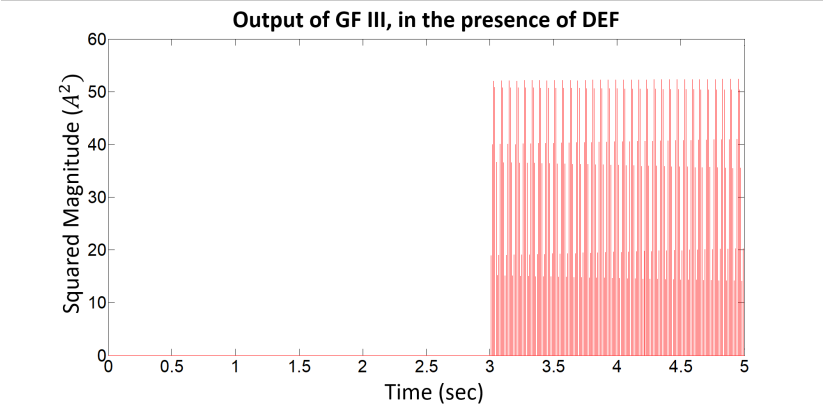

Fig. 6. The output of GF III, in the presence of DEF

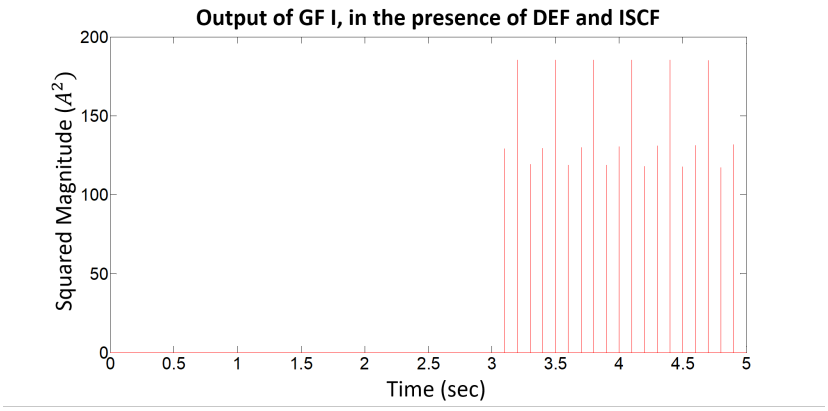

Fig. 7. The output of GF I, in the presence of both DEF and ISCF

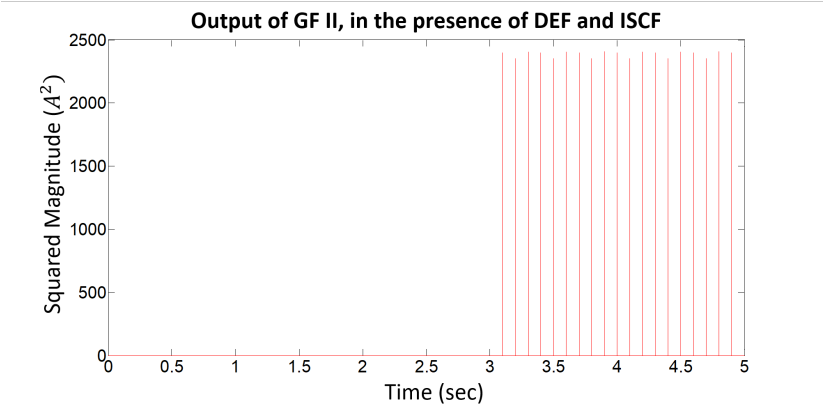

Fig. 8. The output of GF II, in the presence of both DEF and ISCF

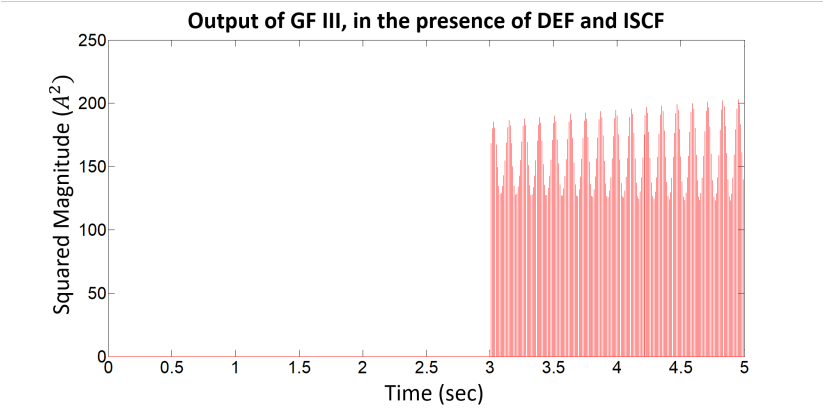

Fig. 9. The output of GF III, in the presence of both DEF and ISCF

The stimulus signal for the bank of GFs was made of the residuals computed between the simulated currents and an EKF. In [9], the authors showed that the spectrum of these residuals remains constant when the wind speed changes.

7. **Conclusions and Perspectives**

The Goertzel Filter was proved to be a candidate to perform MCSA. It was tested on a simulated PMSG of a GWT. It was capable to highlight the effect of the most common faults of such a generator: demagnetization, eccentricity and inter-turn short circuit.

Moreover, a short summary was given on a possible method used to estimate the covariance matrix of the process noise. This covariance matrix is necessary for the implementation of a Kalman Filter. The EKF was used,

in this work, to generate residuals between the simulated and the estimated currents. These residuals were the input of the Goertzel Filters.

Pre-defined thresholds still need to be defined, to be compared against the output of each Goertzel filter. However, these limits are relatively easily set since the output of the GF changes by at least one order of magnitude.

The next step in this research is to apply this method on a real test bench. A DC motor is used to turn the rotor of a stepper motor. The former one acts as a generator.

Another possible step is to refine the method used to estimate the process noise covariance matrix. The current method is subjected to rather strict constraints, which may not always hold in practice.

Acknowledgement

The work has been funded by the Operational Programme Human Capital of the Ministry of European Funds through the Financial Agreement 51675 of 09.07.2019, SMIS code 125125.

REFERENCES

[1] K. Alameh, N. Cité, G. Hoblos, and G. Barakat. Vibration-based Fault Diagnosis Approach for Permanent Magnet Synchronous Motors. *IFAC-PapersOnLine*, 48(21):1444–1450, Sept. 2015.

[2] M. Bocca, J. Toivola, L. M. Eriksson, J. Hollmén, and H. Koivo. Structural Health Monitoring in Wireless Sensor Networks by the Embedded Goertzel Algorithm. In *IEEE/ACM Second International Conference on Cyber-Physical Systems*, pages 206–214, Apr. 2011.

[3] J. Burkholder. Online Covariance, 2013.

[4] J. Faiz and H. Nejadi-Koti. Demagnetization fault indexes in permanent magnet synchronous motors—an overview. *IEEE Transactions on Magnetics*, 52(4):1–11, apr 2016.

[5] G. H. B. Foo, X. Zhang, and D. M. Vilathgamuwa. A Sensor Fault Detection and Isolation Method in Interior Permanent-Magnet Synchronous Motor Drives Based on an Extended Kalman Filter. *IEEE Transactions on Industrial Electronics*, 60(8):3485–3495, aug 2013.

[6] Z. Gao, P. Reviriego, X. Li, J. A. Maestro, M. Zhao, and J. Wang. A fault tolerant implementation of the Goertzel algorithm. *Microelectronics Reliability*, 54(1):335–337, Jan. 2014.

[7] L. Gliga, H. Chafouk, D. Popescu, and C. Lupu. A method to estimate the process noise covariance for a certain class of nonlinear systems. *Mechanical Systems and Signal Processing*, 131:381–393, sep 2019.

[8] L. I. Gliga, H. Chafouk, D. Popescu, and C. Lupu. Comparison of State Estimators for a Permanent Magnet Synchronous Generator. In *22nd International Conference on System Theory, Control and Computing (ICSTCC)*, pages 474–479, Oct. 2018.

[9] L. I. Gliga, H. Chafouk, D. Popescu, and C. Lupu. Diagnosis of a Permanent Magnet Synchronous Generator using the Extended Kalman Filter and the Fast Fourier Transform. In *7th International Conference on Systems and Control (ICSC)*, pages 65–70, Oct. 2018.

[10] L. I. Gliga, B. D. Ciubotaru, H. Chafouk, D. Popescu, and C. Lupu. Fault Diagnosis of a Direct Drive Wind Turbine Using a Bank of Goertzel Filters. In *2019 6th International Conference on Control, Decision and Information Technologies (CoDIT)*, pages 1729–1734. IEEE, apr 2019.

[11] G. Goertzel. An Algorithm for the Evaluation of Finite Trigonometric Series. *The American Mathematical Monthly*, 65(1):34–35, Jan. 1958.

[12] I. Idrissi, R. E. Bachtiri, and H. Chafouk. A Bank of Kalman Filters for Current Sensors Faults Detection and Isolation of DFIG for Wind Turbine. In *International Renewable and Sustainable Energy Conference (IRSEC)*, pages 1–6, Dec. 2017.

[13] K. Koziy, B. Gou, and J. Aslakson. A Low-Cost Power-Quality Meter With Series Arc-Fault Detection Capability for Smart Grid. *IEEE Transactions on Power Delivery*, 28(3):1584–1591, July 2013.

[14] S. D. Levy. The Extended Kalman Filter: An Interactive Tutorial for Non-Experts, 2016.

[15] R. Lyons. Correcting an Important Goertzel Filter Misconception - Rick Lyons, July 2015.

[16] O. O. Ogidi, P. S. Barendse, and M. A. Khan. Fault diagnosis and condition monitoring of axial-flux permanent magnet wind generators. *Electric Power Systems Research*, 136:1–7, jul 2016.

[17] W. Qiao and D. Lu. A Survey on Wind Turbine Condition Monitoring and Fault Diagnosis—Part I: Components and Subsystems. *IEEE Transactions on Industrial Electronics*, 62(10):6536–6545, Oct. 2015.

[18] D. Reljic, J. Tomic, and Z. Kanovic. Application of the Goertzel's algorithm in the airgap mixed eccentricity fault detection. *Serbian Journal of Electrical Engineering*, 12(1):17–32, Feb. 2015.

[19] A. Sapena-Bano, . Kanović, J. Burriel-Valencia, J. Martinez-Roman, J. Perez-Cruz, R. Puche-Panadero, M. Riera-Guasp, and M. Pineda-Sanchez. Using the Goertzel Algorithm Over Disjoint Narrow Frequency Bands for Fault Diagnosis of Induction Motors. In *13th International Conference on Electrical Machines (ICEM)*, pages 1965–1971, Sept. 2018.

[20] P. Sysel and P. Rajmic. Goertzel algorithm generalized to non-integer multiples of fundamental frequency. *EURASIP Journal on Advances in Signal Processing*, 2012(1), Dec. 2012.

[21] Q. Zhang, L. Tan, and G. Xu. Evaluating transient performance of servo mechanisms by analysing stator current of PMSM. *Mechanical Systems and Signal Processing*, 101:535–548, feb 2018.